11th Australasian Fluid Mechanics Conference
University of Tasmania, Hobart, Australia
14-18 December 1992

MULTISCALE ANALYSIS OF ORGANISED MOTION IN TURBULENT SHEAR FLOW

D.K. BISSET and R.A. ANTONIA

Department of Mechanical Engineering
University of Newcastle, NSW 2308, AUSTRALIA

ABSTRACT

A method of decomposing a fully turbulent shear flow into several types of organised motion of different scales is developed. The organised motions account for virtually all momentum transfer, but nearly half of turbulent energy comes from other "random" motion. Results are given for a plane far-wake and a flat plate boundary layer.

INTRODUCTION

Most quantitative studies of organised motion in turbulent shear flows have considered only one particular form of organised motion in a given flow. In most cases, however, the turbulent motion not directly connected with the particular organised motion of primary interest is described as "incoherent turbulence" (Hussain, 1986) or similar, i.e. random and/or uncorrelated motion, and it is not studied in any detail. A few authors have observed the distribution of the incoherent turbulence relative to the primary organised motion (e.g. Hussain, 1986; Antonia et al, 1987; Kiya and Matsumura, 1988), but in spite of the fact that they all indicate that the incoherent turbulence makes greater contributions to quantities such as velocity variances and Reynolds shear stress and heat fluxes than does the primary organised motion, there has been little (if any) attempt to consider whether the incoherent turbulence includes any other type of organised motion.

The approach taken here is to assume that a turbulent shear flow could be organised at all scales. Truly random fluctuations that contribute to turbulent energy may be present simultaneously, but their randomness (or lack of correlation over time and distance) precludes their contributing to shear stress and heat fluxes. Thus the general aim is to find a small number of types of organised motion that convey all of the Reynolds shear stress in a given flow. One simple way of finding this series of organised motions is to work with a detection algorithm that is scale sensitive, and to apply it repeatedly to the data with different settings of the scaling parameter.

It is important to recognise that the individual instances of coherent motion detected in the data will cover a continuous range of scales, and consequently there is a certain arbitrariness in choosing the series of organised motions. In effect, one designs the series of organised motions in terms of both form (via the choice of detection method) and scale, and then determines which type is the best representative of each instance of coherent motion in the flow. The conditional averaging process then guarantees that the actual characteristics of each type of organised motion are suitable for the many instances of coherent motion that it represents. The extent to which the whole series of organised motions represents the flow is determined by subtracting the appropriate organised motion (conditionally averaged) from the data signals for one wavelength around each detection point, and then analysing the signals that remain after all subtractions.

A major motivation for the present multiscale analysis is to provide the basis for certain types of flow modelling. The first stage of modelling is to see whether a turbulent flow, including its spectral and transport properties, can be modelled kinematically by a small group of analytical/numerical model structures, the design of the latter being based on the experimentally determined organised motions. In the long run the idea is to develop a reasonably economical dynamic model of the flow along similar lines that correctly predicts flow properties.

DEFINITIONS AND METHODS

The data used here are two-dimensional in the mean, and the x, y and z co-ordinates correspond to the downstream, transverse (mean shear) and spanwise (homogeneous) directions respectively. Velocity vector components are U, V and W; they are decomposed into mean values and fluctuations as usual, e.g. $U = \overline{U} + u$.

The window average gradient (WAG) method (Bisset et al., 1990) is used for detection. In its basic form, a computation window of length $2\tau + 1$ samples is moved through the digital time series of a given data signal (e.g. u_i, $i = 1, 2, ..., n$), and the WAG function

$$\mathrm{WAG}_i = \frac{S}{2\tau}\left(\sum_{m=i+1}^{i+\tau} u_m - \sum_{m=i-\tau}^{i-1} u_m\right) \quad ,$$

where $S = \pm 1$ is the slope and τ is the scale parameter, is calculated at each point. A detection point d_j is the value of i, within any continuous range of i values where $\mathrm{WAG}_i > 0$, for which WAG_i is largest, provided that $\mathrm{WAG}_i > ku'$ where k is a threshold and the prime indicates rms value. In the present work, $S = +1$ for detections in u signals and $S = -1$ for detections in v. The multisignal WAG detection method (applied to the u and v signals from an X-probe in the present case) begins with a set of detection points (as above) from one of the signals, and then, at each d_j the value of WAG for the other signal is calculated. An "average" WAG value is found, e.g. $\mathrm{WAG}_{AV} = 0.5\ (\mathrm{WAG}_u + p\mathrm{WAG}_v)$ where p is a weighting factor. The detection is accepted if $\mathrm{WAG}_{AV} > k_M u'$. In

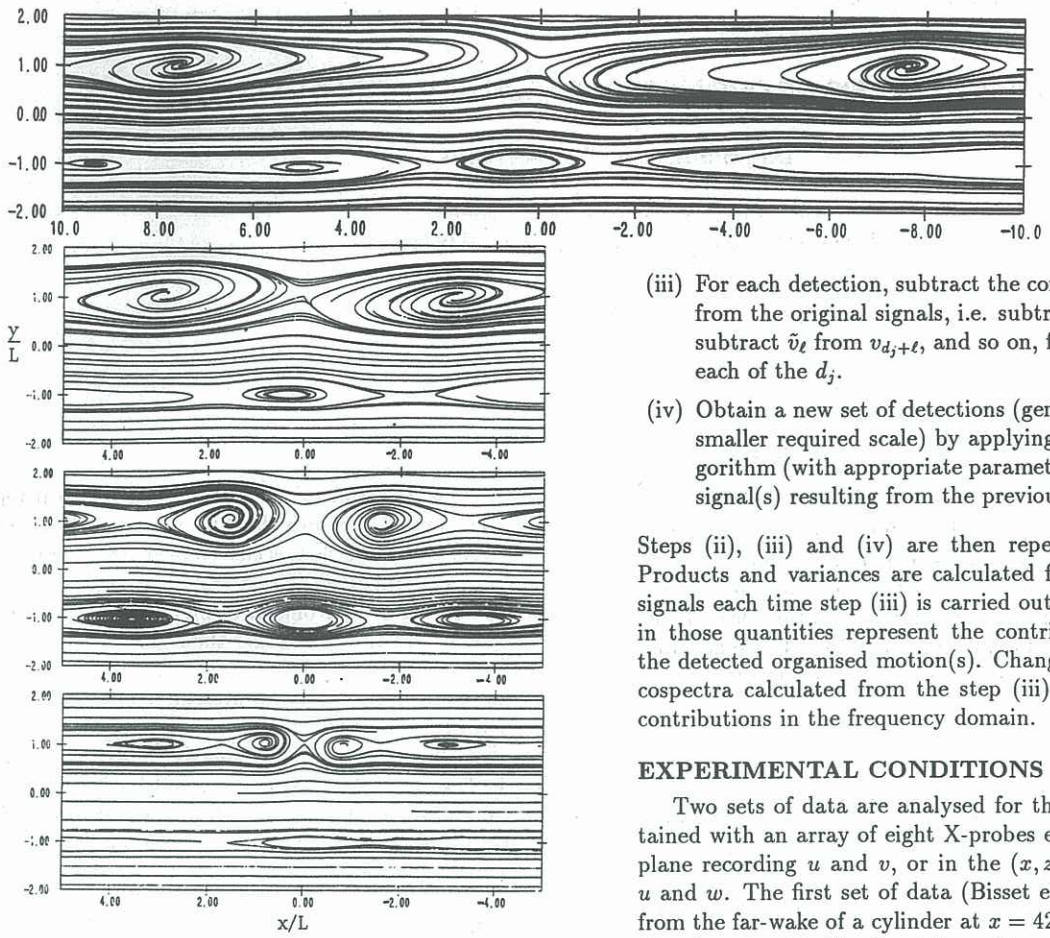

Figure 1 Sectional streamlines from the four detection modes in the far-wake at (x, y) plane, frame of reference $U_c = U_1 - 0.5U_0$. Top to bottom, modes 1–4. Sense of rotation is anticlockwise above centreline, clockwise below.

the present work, all detections are made where $\overline{uv}$ is negative, and $p = -u'/v'$ (initial detections in u signals) or $p = -v'/u'$ (initial detections in v).

Conditional averaging, indicated by <..>, is carried out in the usual way. When a conditional average is regarded as a property of a certain organised motion it is given the special notation $\tilde{u}$, even though $\tilde{u}_\ell \equiv <u>_\ell$. This distinction is important for properties such as the components of the Reynolds shear stress; $\tilde{u}\tilde{v}$ represents the contribution to shear stress made by a particular type of organised motion at a certain point, whereas $<uv>$ is the conditional average of *all* contributions to shear stress at that point.

Sectional streamlines — lines that are always parallel to the velocity vectors in a given plane — are generated with the method described by Bisset et al. (1990).

The steps involved in the multiscale analysis are :

(i) Obtain an initial set of detections (generally beginning at the largest required scale).

(ii) Form the conditional averages of the required signals (e.g. $\tilde{u}_\ell$, $\tilde{v}_\ell$) for $p_1 < \ell < p_2$ where $p_2 - p_1$ corresponds to one period of the particular organised motion. In the present case the magnitudes of p_1 and p_2 are chosen slightly larger, but the values of the conditional averages are smoothly forced towards zero as ℓ approaches p_1 or p_2 : this avoids the possible creation of small discontinuities in the signals resulting from the next step.

(iii) For each detection, subtract the conditional averages from the original signals, i.e. subtract $\tilde{u}_\ell$ from $u_{d_j+\ell}$, subtract $\tilde{v}_\ell$ from $v_{d_j+\ell}$, and so on, for $p_1 < \ell < p_2$ for each of the d_j.

(iv) Obtain a new set of detections (generally at the next smaller required scale) by applying the detection algorithm (with appropriate parameter changes) to the signal(s) resulting from the previous step.

Steps (ii), (iii) and (iv) are then repeated as required. Products and variances are calculated from the modified signals each time step (iii) is carried out, and the changes in those quantities represent the contributions made by the detected organised motion(s). Changes in spectra and cospectra calculated from the step (iii) signals show the contributions in the frequency domain.

EXPERIMENTAL CONDITIONS

Two sets of data are analysed for this work, both obtained with an array of eight X-probes either in the (x, y) plane recording u and v, or in the (x, z) plane recording u and w. The first set of data (Bisset et al., 1990) comes from the far-wake of a cylinder at $x = 420d$ with the array placed symmetrically about the centreplane when parallel to the y axis, and then at $y \approx L$ when parallel to the centreplane. The Reynolds number $R_d \equiv U_1 d/\nu$ is about 1200. (L is the mean velocity halfwidth of the wake, d is the cylinder diameter, U_1 is the free stream velocity and ν is the kinematic viscosity). The second set of data (Antonia et al., 1990) comes from a flat plate boundary layer with zero pressure gradient at a momentum thickness Reynolds number of 2180, but only one result is given here because of space limitations. More extensive results are presented for both flows by Bisset (1992).

RESULTS

It was determined through trial and error that at least four types of organised motion (four detection modes) are required for satisfactory coverage of the uv cospectrum in both flows. Values of the detection parameters are set out in Table I. In the (x, z) plane where no v signals are available, detection is based on u alone with the WAG threshold (k_z in the table) adjusted to give the same detection frequencies as in the (x, y) plane. Parameter values are constant for all y positions. The lengths for which conditional averages are defined, i.e. the ranges of ℓ in steps (ii) and (iii) of the analysis, are 1.33 times the relevant detection window lengths. Setting the thresholds involves a certain amount of experimentation because there is a tradeoff between threshold level and the number of detections. A higher threshold means that the conditional averages have larger magnitudes but they are subtracted from the signals in fewer places. Around 50% to 75% of data points are affected by the subtraction process for each mode, so there are large overlaps between the organised motions.

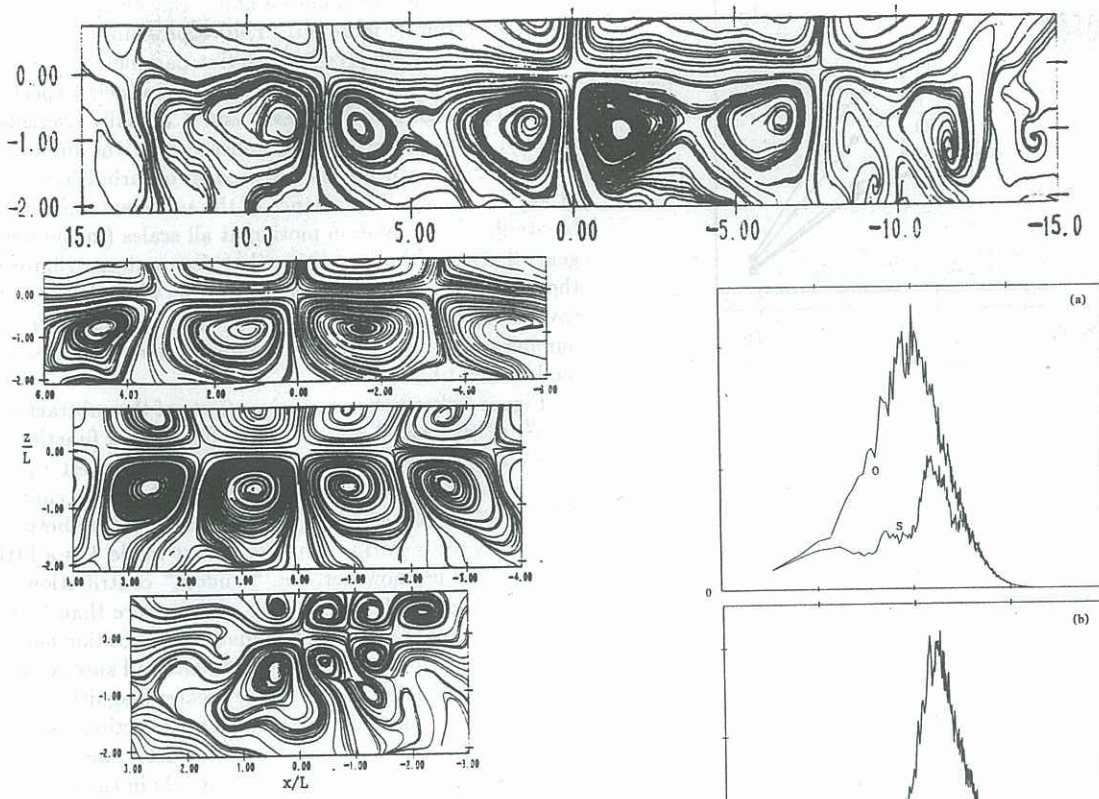

Figure 2 Sectional streamlines in the far-wake (x, z) plane at $y \approx L$ based on WAG u detections, U_c and detection modes as for Figure 1. Note that the x axis is compressed for mode 1.

Table I : Detection parameters

	far-wake				boundary layer		
mode	$(2\tau+1)$	k_1	k_M	k_z	$(2\tau+1)$	k_1	k_M
1	15.5	0.15	0.15	0.25	3.98	0.15	0.25
2	6.1	0.15	0.25	0.34	1.86	0.15	0.25
3	3.0	0.40	0.20	0.41	0.87	0.25	0.25
4	1.1	0.40	0.20	0.40	0.35	0.25	0.25

The averaging window $(2\tau+1)$ is normalized by $f_s L/U_1$ (far-wake) or $f_s \delta/U_1$ (boundary layer).

Figure 1 shows sectional streamlines based on the four modes of detection in the far-wake for the X-probe at $y = 0.88L$, as seen from a frame-of-reference convecting at $U_c = U_1 - 0.5U_0$ (where U_0 is the centreline mean velocity defect). The plots all show saddle points with vortex-like rotating regions upstream and downstream, but the scale and shape of the regions vary greatly with detection mode. For mode 3 there is a vortex-like region on the lower side of the wake directly below the detection points, forming the alternating pattern that is dominant for the large scale organised motion analysed by Bisset et al. (1990). Contour plots of $\tilde{u}$ corresponding to these detections (see Bisset, 1992) are noticeably antisymmetrical for mode 3, whereas $\tilde{v}$ contours spread across both sides of the wake. To some extent the converse is true for mode 1. The $\tilde{u}$ and $\tilde{v}$ contours in general indicate considerable periodicity in the x direction, with the regions of alternate sign tending to follow the scale of the detection mode for some distance beyond the ends of the detection window.

Sectional streamlines at $y \approx L$ in the (x, z) plane are

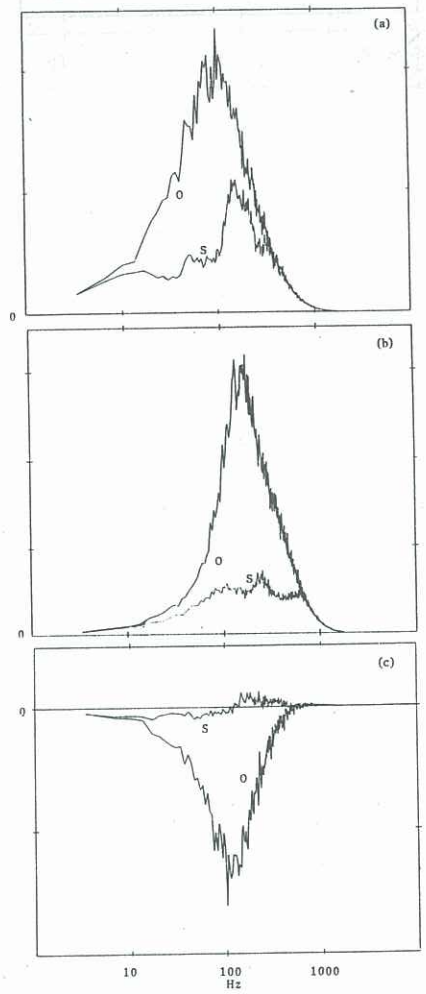

Figure 3 Frequency multiplied power spectra for (a) u and (b) v, and (c) cospectrum of u and v, in the far-wake at $y = 0.88L$; O indicates original function and S indicates function after subtraction of organised motion.

presented in Figure 2. As noted above, the u signal detections in this plane are not ideal, but they do give an indication of the three-dimensional form of the four types of organised motion. Each detection mode results in a pattern of contra-rotating vortex-like regions, but the scales of the regions greatly decrease from mode 1 to mode 4. For mode 2 and especially mode 1 the regions are very elongated in the x direction. Contours of conditional transverse vorticity $\tilde{\omega}_z$ (Bisset, 1992) are aligned quite closely with the streamline patterns for modes 2–4, and even for mode 1 there is significant correspondence. In this plane the organised motions appear to be a series of transverse vortices, whereas the evidence from the (x, y) plane points to a series of spanwise vortices. Thus the basic modules of the organised motions are quite complex.

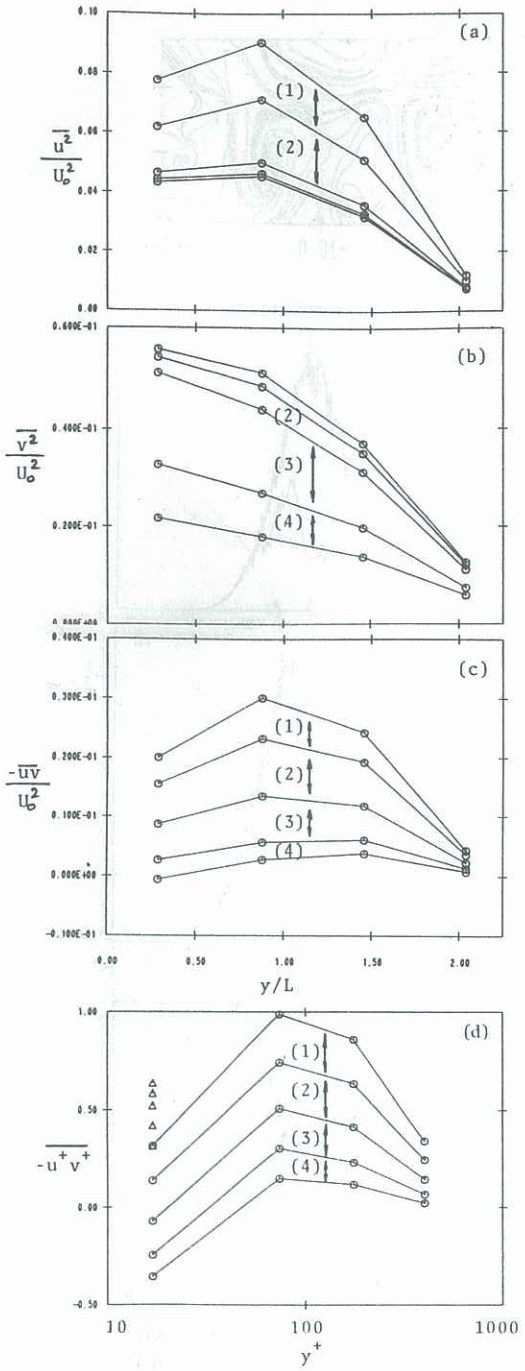

Figure 4 Composition of Reynolds stresses for the far-wake (parts a–c) and boundary layer in terms of successive subtractions of the four modes of organised motion, as indicated by (1) to (4). (a) $\overline{u^2}$; (b) $\overline{v^2}$; (c) $-\overline{uv}$; (d) $-\overline{uv}$ for the boundary layer.

Many results have been obtained for the boundary layer data, some of which were presented by Bisset (1992). For modes 2–4 there are many similarities to the far-wake results, but all results vary with distance from the wall and it is impossible to give details here.

The effects of the subtractions of all organised motions on the power spectra of u and v and on their cospectrum at a point in the far-wake are shown in Figure 3. Results for the boundary layer (except very near the wall) are quite similar. The centre frequencies for modes 1 and 2 show up as dips in the u power spectrum (Figure 3a), while the centre frequencies for modes 3 and 4 can be seen in the v power spectrum (Figure 3b). The cospectrum (Figure 3c) shows that, with the present detection parameters, modes 1 and 2 capture a high proportion of $\overline{uv}(f)$ in their respective frequency ranges, and modes 3 and 4 actually overshoot slightly. The power spectra indicate that the organised motions do not capture the full amount of turbulent energy at any frequency. The balance of the turbulent energy can be attributed to random motion at all scales (in the fairly general sense of being motion that does not contribute to the overall momentum transfer). In flows where the spectra cover a greater range of frequencies, and at higher Reynolds numbers, it is likely that a greater number of detection modes would be required.

Figure 4 shows the successive effects of the subtractions on $\overline{u^2}$, $\overline{v^2}$ (far-wake) and $\overline{uv}$ (both flows) as a function of y. Except at the boundary layer position nearest to the wall, it can be seen that the four types of motion capture 85%–100% of $\overline{uv}$ between them. The distribution between the four types is fairly even except that mode 4 is a little weaker. For $\overline{v^2}$, however, the "random" contribution (of order 40%) is significant, and for $\overline{u^2}$ it is more than 50%.

The $\overline{uv}$ results from the boundary layer position closest to the wall are interesting in that $\overline{uv}$ after all subtractions has changed sign and has a slightly greater magnitude than the original (Figure 4d). Although the detection parameters are unchanged in y, there are fewer detections here for each mode, the reduction occurring mainly in the multisignal step where u and v are both important. In spite of this, the cospectrum here (not shown) becomes distinctly positive at nearly all frequencies. The possibility that some organised motions make *positive* contributions to $\overline{uv}$ was investigated by returning to the original signals and making a series of detections exactly as before except for a *positive* weighting factor at the multisignal WAG stage. There are even fewer detections in each mode than with a negative weighting factor, but their effect on $\overline{uv}$ is still significant. The successive *increases* in $-\overline{uv}$ as the four modes are subtracted are indicated by the triangles in Figure 4d. The increases here would almost exactly be balanced by the excessive decreases resulting from the first set of subtractions. Thus it appears that the reduction in momentum transport close to the wall (at least from the point of view of the present analysis) is mainly caused by an increase in the number and strength of motions of the wallward interaction type rather than a decrease in the strength of ejection-type motions.

ACKNOWLEDGEMENT

The support of the Australian Research Council is gratefully acknowledged.

REFERENCES

ANTONIA, R. A., BISSET, D. K. and BROWNE, L. W. B. (1990) *J. Fluid Mech.*, **213**, 267-286.

BISSET, D. K. (1992) Ph.D. Thesis, University of Newcastle, Australia.

BISSET, D. K., ANTONIA, R. A. and BROWNE, L. W. B. (1990) *J. Fluid Mech.*, **218**, 439-461.

HUSSAIN, A. K. M. F. (1986) *J. Fluid Mech.*, **173**, 303-356.

KIYA, M. and MATSUMURA, M. (1988) *J. Fluid Mech.*, **190**, 343-356.